Scientific Research Publishing

Open Journal of Applied Sciences, 2025, 15(12), 3843-3864
https://www.scirp.org/journal/ojapps
ISSN Online: 2165-3925
ISSN Print: 2165-3917

# Electrodynamics of the Earth's Magnetosphere at High Latitudes: Geomagnetic Storm Case's of June 22/23, 2015

**Inza Gnanou[1,2*], Salfo Kabore[2,3], Abidina Diabate[2,4], Christian Zoundi[2,3], Doua Alain Gnabahou[2,3], Frédéric Ouattara[2,3]**

[1]Département de Physique, École Normale Supérieure (ENS), Koudougou, Burkina Faso
[2]Laboratoire de Chimie Analytique, de Physique Spatiale et Énergétique (LAC@PSE), Koudougou, Burkina Faso
[3]Département de Physique, Université Norbert ZONGO (UNZ), Koudougou, Burkina Faso
[4]Département de Physique, Université Nazi Boni, Bobo-Dioulasso, Burkina Faso
Email: *gnanouinza@gmail.com

**How to cite this paper:** Gnanou, I., Kabore, S., Diabate, A., Zoundi, C., Gnabahou, D.A. and Ouattara, F. (2025) Electrodynamics of the Earth's Magnetosphere at High Latitudes: Geomagnetic Storm Case's of June 22/23, 2015. *Open Journal of Applied Sciences*, **15**, 3843-3864.
https://doi.org/10.4236/ojapps.2025.1512249

**Received:** August 25, 2025
**Accepted:** December 6, 2025
**Published:** December 9, 2025



## Abstract

Geomagnetic storms are generally the main source of interplanetary and geomagnetic disturbances, constituting a major natural hazard due to their potential to damage technological and electrical systems, on which our society is heavily dependent. On June 22 and 23, 2015, our magnetic shield was impacted by the second strongest storm during the solar maximum of solar cycle 24, propelling a series of interplanetary coronal mass ejections (ICME_1 and ICME_2) towards Earth. Based on observational data derived from ground-based magnetometers (BOX and DRV) and spacecraft (WIND, ACE, SDO, and SOHO), we are investigating the high-latitude dynamics of the Earth's magnetospheric cavity as it was impacted by this series of extreme events. Our results show that the events of June 22-23, 2015, associated with violent storms with strong and prolonged main phases, radically altered the behavior of the inner magnetosphere. While ICME_1 was characterized by fairly calm weather upstream, ICME_2 produced strong storm effects at high latitudes. In addition, analysis of data collected at one-minute intervals highlights that the dynamics of magnetospheric plasma correlate with solar wind intensity depending on the period and phase of the storm. In general, while it appears that the East/West directions of the $E_M$ field are associated with the orientation of the IMF-$B_z$, $E_M$ field variability becomes more pronounced and direct in polar regions when solar winds interact with the geomagnetic field. During the main storm phase, $E_M$ field intensifies in the dawn-dusk sector of the Earth's magnetosphere for a south-facing IMF-$B_z$, while a north-facing IMF-$B_z$ orientation is associated with a weakening of $E_M$ field in the dusk-dawn sector of the magnetospheric

cavity during the storm recovery phase. The results presented in this paper are likely to be important for Global Navigation Satellite System (GNSS) and weather forecasting applications.

## Keywords

Superstorms, Interplanetary Coronal Mass Ejections, Magnetosphere, Geomagnetic Field, Solar Wind

## 1. Introduction

Nowadays, the existence of various phenomena such as solar flares, coronal mass ejections (CMEs), and geomagnetic storms helps to understand Sun-Earth events. From previous studies [1] [2], geomagnetic storms are the most important component of space weather impacts on Earth. Observations of solar events on the ground and in interplanetary space reveal that a geomagnetic storm can be considered as an event in which disturbances are triggered by solar flares. A geomagnetic storm is defined as a large-scale, abrupt disturbance of the Earth's magnetic field caused by the interaction of intense solar winds with the Earth's magnetosphere. Geomagnetic storms can also generate ionospheric storms. It is well known that one of the possible causes of these geomagnetic events lies in solar flares, which are huge explosions of harmful electromagnetic radiation from the Sun's active regions. In general, solar flares occur when the Sun's intense magnetic fields become too entangled. These powerful blasts of magnetic plasma erupted by the Sun travel at millions of kilometers per hour through interplanetary space, interacting with our planet's protective magnetic shield: the Earth's magnetosphere. Violent eruptions can physically affect humans on Earth [3]-[5]. They can also cause potentially fatal power outages, damage to technological systems such as satellites, radio communication failures, and navigation problems [2] [6]-[8]. These disturbances, whether natural or man-made, can occur in both calm and disturbed geomagnetic conditions. However, the most significant magnetospheric alterations are caused by geomagnetic storms/storms when the magnetosphere is strongly disturbed on a global scale.

Since 1859, violent flares that could wreak havoc on Earth had been discovered before other active processes on the Sun. However, disturbances of the solar wind and Earth's magnetosphere were linked only to solar flares. Later, in the early 1970s, other powerful processes of solar origin, such as coronal mass ejections (CMEs), were discovered. However, [9] significantly changed the situation, and today there is a broad consensus that geomagnetic disturbances can be caused by several sources, including corotation interaction regions (CIRs), magnetic clouds, and CMEs (see, for example, [10] [11]). CMEs often accompany solar flares, although scientists are still trying to determine exactly what the undeniable link is between these two magnetic phenomena. It is well known that CMEs significantly

control space weather [12]-[14]. From sources located in the Western Hemisphere, CMEs originating near the central meridian of our star and heading towards Earth are the most geo-effective. Given their significant influence on our terrestrial environment in a variety of ways, it would be very useful to look into space weather forecasting (geomagnetic storms, effects on navigation/communication systems, risks for astronauts, etc.). That said, solar and interplanetary events play an important role in understanding the complex solar wind/magnetosphere system. While it seems that magnetosphere and ionosphere interact crucially during strong geomagnetic storms [15]-[17], to our current knowledge, recent work on the nature of this interaction only addresses the ionized—ionospheric—part of the terrestrial environment (see, for example, [18]-[21]). In this study, our particular focus will be on the magnetospheric cavity during violent storms associated with CMEs.

CMEs are dynamically expelled and driven by coronal magnetic fields, which diminish as they pass through interplanetary space, where other processes can accelerate them. Thus, CME/solar wind interaction can provide the drag necessary for the acceleration/deceleration of CMEs as a function of their velocity, and the increase in this magnetic drag constitutes a major obstacle for spacecraft during their motion. Observations of CME by SOHO/LASCO and ground-based measurements of interplanetary CME (*i.e.*, ICME) have highlighted the main causes of geomagnetic storms. If the counterparts of ICME have a significant meridional component of the interplanetary magnetic field (IMF), then after reaching the Earth's magnetosphere, they can lead to geomagnetic storms [22] [23]. According to [24]-[26], a storm occurs after a very calm day preceded by a period of development during which the IMF turns southward ($B_z < 0$) with an increase in the energy density of the solar wind plasma near the Earth. Previous studies have classified storms according to the values of the horizontal component of the magnetic field (SYM/H) and their temporal variations in four geomagnetic conditions [27] [28]. More in-depth discussions of recent storm classification can be found in review articles by [29]-[33].

According to [34], geomagnetic disturbances due to the interaction between solar winds and the Earth's magnetosphere are known to strongly influence electrodynamics during violent geomagnetic storms. The storm-time electrodynamics of the Earth's magnetosphere are considerably altered compared to calm-weather behavior due to additional disturbances caused by magnetospheric convection electric fields (e.g., [35] [36]). During geomagnetic storms, the magnetospheric convection electric field—the interplanetary electric field mapped at high latitude—penetrates rapidly to the equator as a fast-penetrating electric field (PPEF) with eastward and westward polarities during the day and night, respectively (e.g., [35] [37]-[42]). Two mechanisms are responsible for the generation of electrodynamic effects on the magnetosphere during a thunderstorm. The first mechanism is PPEF penetrating electric fields [25] [40] [43]-[46] and the second, disruptive dynamoelectric fields [40] [45] [47]. According to several studies, such as [48], the

main driver of storm weather effects in the upper ionosphere (*i.e.*, magnetosphere) is the PPEF. PPEF is a local, transient disturbance, while a magnetospheric convection electric field ($E_M$) is a large-scale electric field resulting from the interaction of the solar wind with the Earth. The PPEF and $E_M$ field are linked by the mutual influence of their effects on plasma and magnetospheric dynamics. During intense geomagnetic storms, the PPEF can disrupt and modify the $E_M$ field. For example, a strong PPEF can lead to an increase in convection velocity, thus modifying the shape and dynamics of the magnetosphere. Conversely, the $E_M$ field can influence the propagation and duration of PPEFs. The study of these phenomena is crucial to understanding the impact of geomagnetic storms and disturbances in the space environment. In this study, particular attention will be paid to the convective electric field that causes various types of global and local electrodynamic responses in the inner magnetosphere. Despite many efforts made in recent deployments of ground- and space-based instruments (see, for example, [18] [49]-[56], the behavior of the magnetosphere during violent storms is not yet well elucidated. The main challenge here is to present a global overview of the interplanetary electric/magnetic field conditions in order to understand the magnetospheric cavity response during the violent storm of June 22/23, 2015. Note that June 22/23, 2015, included a period of calm weather and a disturbed period associated with the arrival of two interplanetary shocks in the early morning and twilight of June 22. Clearly, the storm of June 22/23 2015 was not the strongest of solar cycle 24 compared with that of St. Patrick's in March 2015, however, the choice of this storm is motivated by its notable effects on radio communications, its large amount of mass ejected by the solar corona, the intensity of its moderate to severe impact on the Earth's magnetosphere, and so on.

In June 2015, a series of interplanetary coronal mass ejections (ICMEs) appeared to originate from the Sun's active AR 2371 region (**Figure 1(a)**). These were subsequently recorded by NASA's Advanced Composition Explorer (ACE) satellite, located on the Sun-Earth line at a distance of around 1% of the Earth-Sun distance, as abrupt enhancements in solar wind speed and density. Note also that there have been episodes of large-scale disturbances on the western side of AR 2371 (more precisely in the AR 2367 region) that have not had associated CME, probably because they were not large enough to become halos. The impact of these ICMEs on the Earth's magnetosphere resulted in a violent G4-class geomagnetic storm (*i.e.*, M6.5-class solar flare) on June 22/23, 2015, as shown in **Figure 1(b)**. In addition to large auroras and a radio signal blackout in several Nordic countries, the June 2015 storm produced a significant compression of the upstream of the Earth's magnetosphere, reducing it to 11 Earth radii $R_T$ ($1R_T = 6371$ km). Although solar flares can be visible in white light, they are often more easily noticed thanks to their luminous X-ray and ultraviolet emissions. Fortunately, the unsuspected June 22/23 event lasted only a few hours and had only minor consequences on our planet Earth. This example is a reminder of how important it is to study the impact of geomagnetic storms so as to be able to prevent solar flares and, in this way, pre-

pare for them to avoid planetary chaos in our societies, which have become highly dependent on electricity, radio exchanges, satellites, and so on. This article is organized as follows: first, the data set and methodology adopted are introduced in section 2, followed by the choice of empirical model organized according to the $E_y$ electric field frozen in solar winds. Next, Section 3 describes our results and various interpretations. And finally, a conclusion is presented in Section 4.

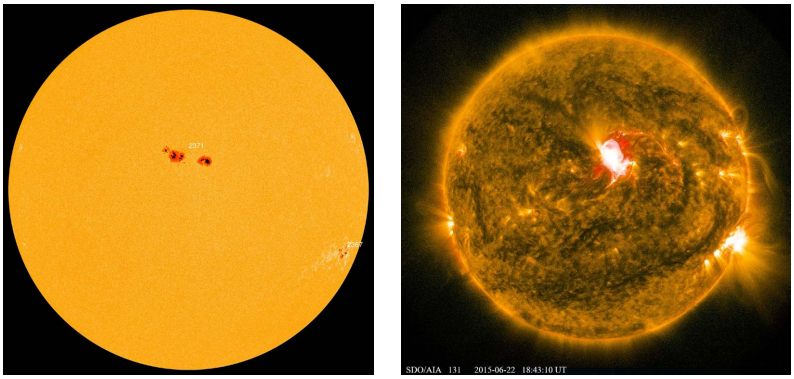


(a) (b)

**Figure 1.** Flare and sunspot of June 22, 2015. (a) Sunspot AR2371. Credit: SDO/HMI; (b) M6.5-class solar flare on June 22, 2015, at 18:43 UT. Credit: NASA/SDO.

## 2. Data and Methodology

In this study, high-throughput data from solar events on June 22 and 23, 2015, include observations of solar wind variables and magnetic indices. On the one hand, geophysical and interplanetary (solar geocentric and magnetospheric coordinate system (GSM)) parameters from the WIND spacecraft orbiting the L1 Lagrange point are compiled by the space science community and made available via the OMNIWeb system. On the other hand, it is well known that ground-based magnetic observations offer excellent spatial and temporal coverage for statistical studies. Ground-based magnetic data are therefore crucial for a number of applications, including monitoring the evolution of geomagnetic storms and space weather. In addition to the geomagnetic indices (Dst, Kp, and AE) extracted from the International Magnetic Index Service ISGI "http://isgi.unistra.fr/", definitive ground observation data "http://www.bcmt.fr/data_download.php" come from two magnetometers close to the Earth's magnetic poles and located at high geomagnetic latitudes (latitudes > 50˚). Since key geomagnetic indices such as Dst and SYM/H are derived from low-latitude magnetometer stations, the choice of high latitudes (both BOX and DRV) is justified by the fact that the strong interactions of the solar wind/magnetosphere system are particularly evident at auroral latitudes. An overview of the location of the BOX and DRV observatories is shown in **Figure 2**. The BOX magnetometer is located in the Northern Hemisphere (58.07˚N, 38.23˚E) at Borok, Russia, and the DRV magnetometer is located in the Southern Hemisphere (66.665˚S, 140.007˚E) at Dumont-d'Urville on the Antarctic coast of France. The scalar FS and vector FV 1-minute cadence functions (values) of BOX

and DRV are calculated from the 5-second numerical values using a minute-centered Gaussian function (http://www.bcmt.fr/). FV, due to convection currents in the Earth's liquid outer core, is characterized by intensity, direction, and sense at each point in space, while FS is mainly represented by the total intensity of the geomagnetic field.

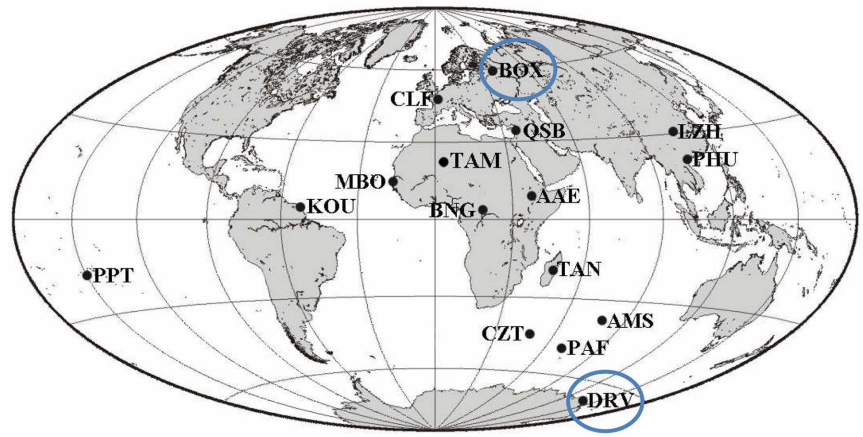


**Figure 2.** Observatory locations (source: taken from data catalogue N˚27 (2005), published by the World Data Center for Geomagnetism, Kyoto).

In addition, the high-latitude dynamics of magnetospheric plasma have been interpreted via the frozen electric field $E_y$ in solar winds. $E_y$ ($E_y = -V_{sw} \times B_z$) is the main factor determining the structure of the inner magnetospheric electric field and the associated plasma convection processes. In this study, the magnetospheric convection electric field $E_M$ ($E_M = 0.13E_y + 0.09$) was determined by the $E_y$ electric field transformation law frozen in the solar wind. For more details on the determination of $E_M$ field, please refer to [57] [58]. During geomagnetic storms, $E_M$ field plays a crucial role in transporting charged particles (from solar wind) from magnetosphere's tail to the front and injecting energy, which can cause significant disturbances. Because of the persistent statistical approach adopted in this manuscript, each geophysical and interplanetary data item is carefully examined to remove any aberrations related to the surprisingly large discrepancies. Only cases where solar and magnetic parameters were available simultaneously were taken into account in this study, *i.e.*, 87% of the raw data for the period June 22-23, 2015.

## 3. Results

### 3.1. Geomagnetic Storms of June 22 and 23, 2015

In this section, we discuss the time-corrected variations over one-minute cadences of various interplanetary plasma parameters of the unusual event dated June 22 to 23, 2015, during the maximum phase of solar cycle 24. Indeed, from June 22 (white background in **Figure 3**) to June 23 (orange-ish background in **Figure 3**) of 2015, a series of geomagnetic storms was broadcast by large polar aurorae, causing a radio signal blackout on Earth. Mainly caused by solar flares, these extraordinary

events eject charged particles into space in the form of coronal mass ejections (CMEs) or their counterpart, interplanetary coronal mass ejections (ICMEs). As ICMEs cross the Earth's magnetosphere and interact with the solar wind in the background [59] [60], it would be necessary to monitor the evolution of solar wind parameters and magnetic indices. Panels (a)-(c) in **Figure 3** show temporal variability in 1-minute steps of near-Earth solar wind parameters in Geocentric Solar Magnetospheric (GSM) coordinates at L1 Lagrangian point and magnetic indices from June 22 to 23, 2015. These panels show how the onset of an intense geomagnetic storm took place in the early morning of June 22, when two asymmetrical full-halo interplanetary shocks struck Earth's magnetosphere, and how magnetospheric conditions were abruptly altered. According to **Figure 3(a)**, BOX (in the Northern Hemisphere) and DRV (in the Southern Hemisphere) magnetometers on the ground recorded a sudden jump in the magnetic field (Storm Sudden Commencement: SSC) that heralded the arrival of two interplanetary shocks (IS) on Earth at around 05:45 UT and 18:40 UT on June 22, 2015. [61] report that these IS were associated with a series of interplanetary coronal mass ejections (ICME_1 and ICME_2). According to **Figure 3(b)**, these arrivals caused concomitant increases in dynamic pressure (red curve) and solar wind velocities (black curve). As a result of these synchronized increases across the shock, the ram pressure of the solar wind exerted on the Earth's magnetosphere abruptly compressed the upstream magnetosphere while generating eastward magnetopause electric currents and positive jumps in the horizontal component of the Earth's magnetic field (SYM/H), as can be seen in **Figure 3(d)**, red curve. It is well known that magnetic field variations observed on the ground are highly dependent on the latitude of the magnetic observatory. Low-latitude observatories clearly see the SSC and main phase of a magnetic storm. On the other hand, those at high latitudes see the first SSC, followed by a series of substorms. **Figure 3(a)** shows the difference in vector FV and scalar FS values of the total intensity of the Earth's magnetic field from BOX and DRV located at high latitudes 58.07˚North and 66.67˚South, respectively. FV-FS difference shows that the event of June 22/23, 2015 was felt more on the northern side of the hemisphere, with a not sufficiently clear response (*i.e.*, lower amplitude) from DRV and a latency of around 62 min from BOX to the arrival of a second ICME (ICME_2). These findings suggest that the source of this series of solar flares is located in the Northern Hemisphere.

During the first event (ICME_1), $B_z$ component of the interplanetary magnetic field (IMF-$B_z$) shifted from north to south, with peaks of 8.99 nT and −9.77 nT, respectively (**Figure 3(c)**, black curve). On average, the dynamic pressure of solar flux was only 7.21 nPa, with a corresponding 12% increase (381 km/s to 427.1 km/s) in velocity. While the $E_y$ electric field frozen in solar wind showed small variations upstream of ICME_1 (**Figure 3(c)**, red curve), dynamic pressure (**Figure 3(b)**, red curve), auroral activity characterized by AE index (**Figure 3(d)**, grey bars) and SYM/H index (**Figure 3(d)**, red curve), all of almost linear characteristics in constant evolution, fluctuated respectively with vigors less than 0.24 Pa, 13.09 nT and

1.07 nT from their mean. However, downstream of this event, the quantities in question showed more moderate variations.

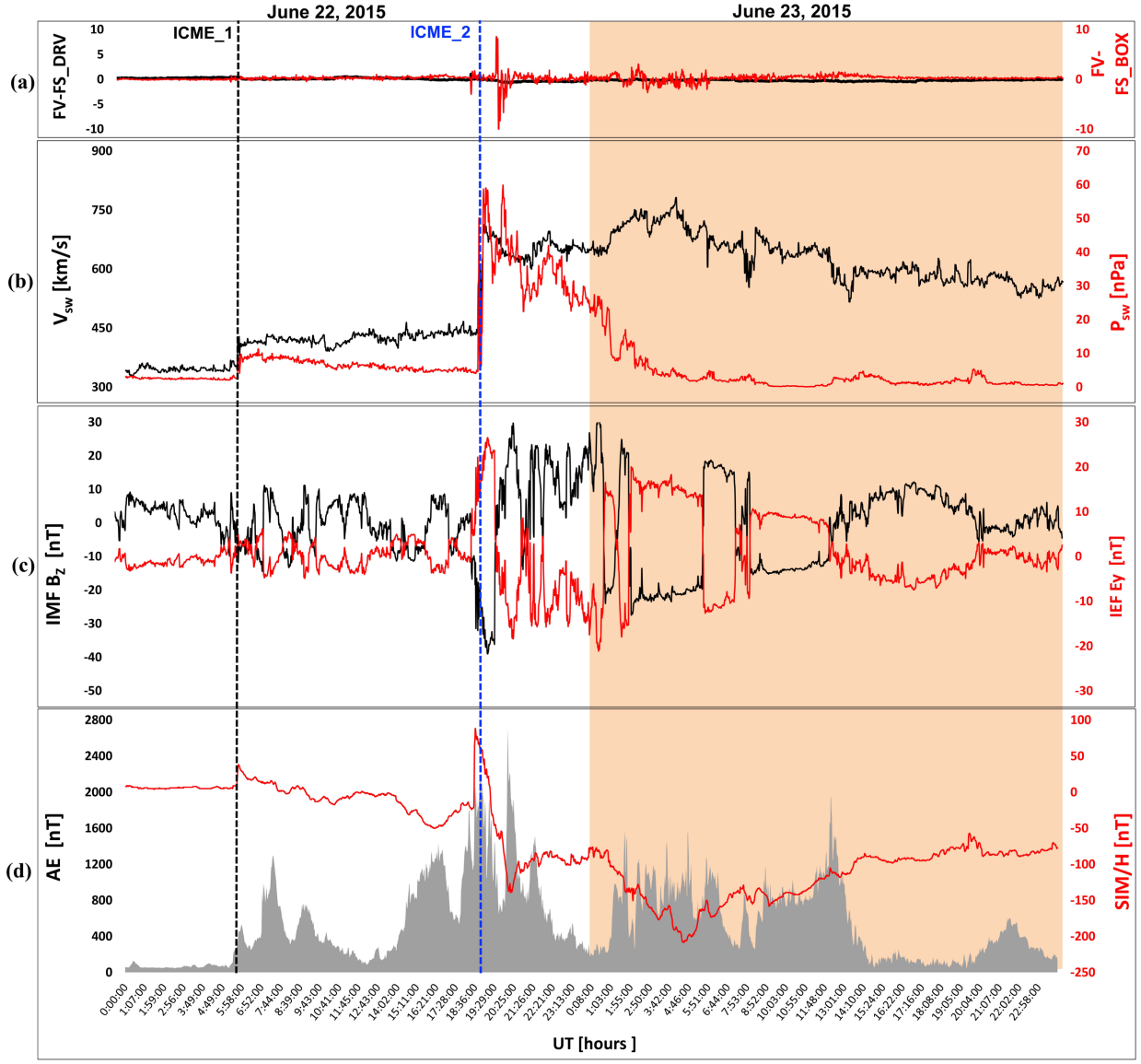


**Figure 3.** Variation in interplanetary and geophysical parameters during the solar events of June 22-23, 2015. (a) FS scalar and FV vector functions of the ground magnetic field; (b) Velocity ($V_{sw}$) and pressure ($P_{sw}$) of the solar wind; (c) Interplanetary magnetic and electric fields; (d) Auroral activity index (AE) and north-south component of the geomagnetic field (IFM-$B_z$). Dotted vertical lines indicate the arrival times of the two interplanetary coronal mass ejections (ICME_1 and ICME_2) that struck the Earth.

Furthermore, on the same date (*i.e.*, June 22, 2015), a second event (ICME_2) was observed at 18:40 UT with significant storm-time changes in solar wind parameters resulting in a positive disturbance of about 88 nT in SYM/H. The event began with a fairly intense IMF-$B_z$ with a predominantly southerly orientation (for around 90 min) of minimum intensity −38.98 nT at 19:23 UT, which is the most negative excursion measured in 2015, before turning sharply northwards. This event is accompanied by a remarkable ~64% variation in solar wind speed

and $\Delta P = 55.75$ nPa increase in dynamic pressure to the southwest. This sudden increase in solar wind pressure compresses Earth's magnetosphere, producing SSC: this is the initial phase of the geomagnetic storm. This increase, according to [62] and [63], is caused by a temporal storm penetration electric field. Downstream of ICME_2, while solar flux dynamic pressure dropped from 92% of its initial value on June 23 at 03:49 UT to remain constant in the ±5.2 nPa range over the rest of the time, solar particle velocity slowly peaks at 781.8 km/s at 03:56 TU, then slowly decays to 516.8 km/s at 13:07 TU. IMF-$B_z$ underwent various storm effects: that is, multiple positive (North) and negative (South) orientations between 01:30 UT and 12:00 UT on June 23, 2015. We consider this effect in our results to be due to the effect of rapid penetration of interplanetary electric fields IEF $E_y$, which is positive on the day side and negative on the night side (see, for example, [64]). Southern orientations of IMF-$B_z$ ($B_z < 0$) confirmed by the ACE spacecraft led to an interconnection between IMF and geomagnetic field lines. The consequence of this interconnection was the significant depression to −208 nT of the SYM/H geomagnetic index around 04:24 UT. This intense storm episode in June 2015 caused spectacular magnetospheric (and therefore ionospheric, since the two systems are closely coupled) variability, which impacted global navigation satellite systems (GNSS) and degraded the performance of the European geostationary overlay navigation service [19] [48] [65]-[69]. This shows how magnetospheric electrodynamics contributes to improving GNSS performance (e.g., attenuation of ionospheric scintillation) or space weather forecasting models [70]-[72].

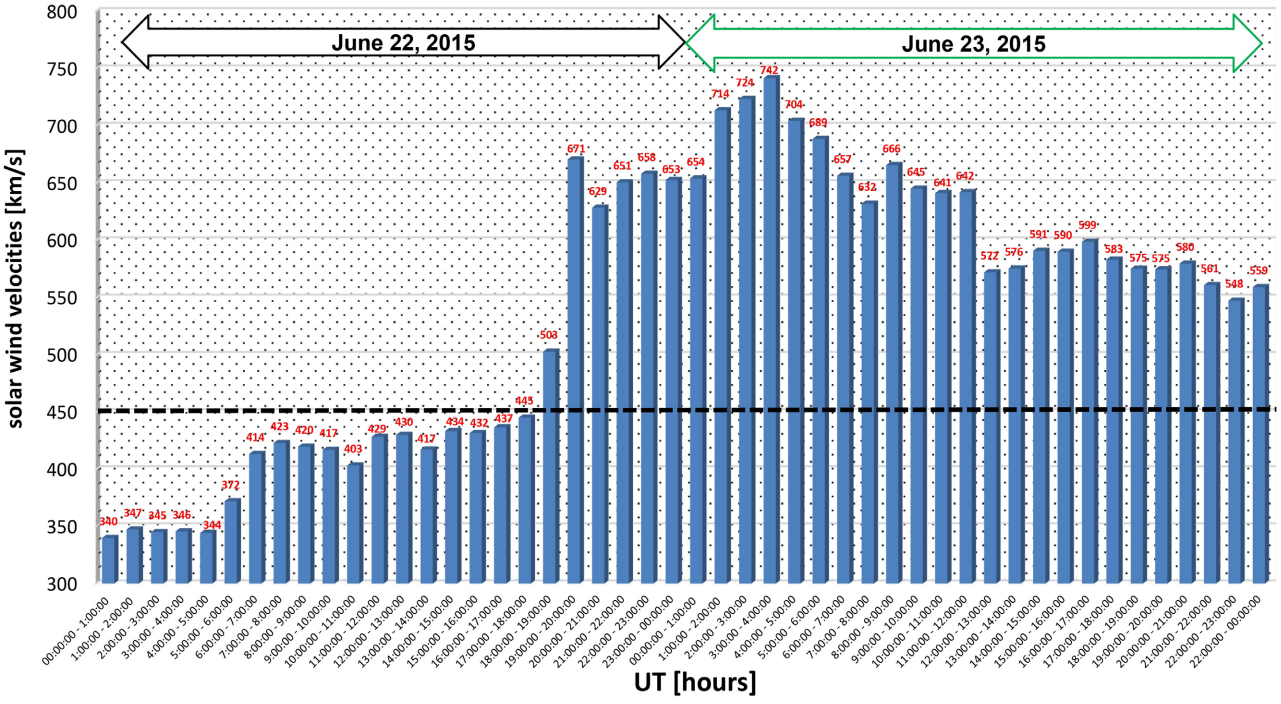


**Figure 4.** Hourly average solar wind velocities from June 22 to 23, 2015.

Additionally, while the AE index reached the limit of 1298 nT at 07:24 TU

downstream of ICME_1, AE exceeded 2000 nT during ICME_2 (**Figure 3(d)**, grey bar). Similarly, solar flux velocity amplitudes during ICME_1 and ICME_2 on June 22 were less significant than those downstream of ICME_2 on June 23, as shown in **Figure 4**. Indeed, in **Figure 4**, by setting the bar at 450 km/s, which would be the minimum amplitude of fast solar wind speeds [60] [73]-[75], we can see that 28.60% (June 22) of the solar flux versus 92.44% (June 23) have minimum amplitudes of 450 km/s. As a result, variations in electrojet index AE (**Figure 3(d)**, grey bar) show that the storm was accompanied by fairly intense auroral activity associated with strong fluctuations between −21.09 and +26.57 mV/m in IEF $E_y$. According to [43] [76] [77], such amplitudes are comparable to extreme storm values. In addition, [78] shows that large IEF $E_y$ values are responsible for violent and intense geomagnetic storms. Moreover, with a predominantly southerly orientation of the IMF-$B_z$ accompanied by strong solar flux surges associated with oscillatory behavior of auroral activity AE reaching 2698 nT on June 22, the series of storms observed on June 22/23, 2015 remains the second most important storm in the 24$^{th}$ solar cycle after the St. Patrick's storm that occurred in March 2015 [18] [61] [79]-[83].

### 3.2. Interplanetary Conditions and Magnetospheric Convection

When ICMEs arrive and interact with the Earth's magnetic field, a series of mechanisms occur in the Earth's magnetosphere, leading to the disturbances observed in the geomagnetic field and magnetosphere [45] [69] [84] [85]. The importance of these mechanisms varies from case to case and phase to phase of a geomagnetic storm. The magnetospheric convection electric field, noted here as $E_M$ [mV/m], is one of the mechanisms causing these strong disturbances, leading to the formation of complex magnetospheric structures, such as the magnetic tail and the aurora borealis. Details of these disturbances are examined in this section. In fact, solar cycle 24 (January 2008-December 2019) saw fewer sunspots than average, but major solar events did occur. For example, as shown in **Figure 5**, on June 22, 2015, two solar corona ejections (ICME_1 and ICME_2) bombarded the Earth's protective cavity. Ring current and response of high-latitude geomagnetic activity, as represented by SYM/H indices and AE auroral electrojet, were discussed in the previous section. Examination of **Figure 3(b)** showed a sudden increase in $V_{sw}$ velocity associated with a sharp jump in plasma dynamic pressure $P_{sw}$ at the shock level at ~18:40 UT. At the same time, flux density (**Figure 5(a)**) increased drastically by ~41% at the sheath (downstream of the shock), and IMF-$B_z$ turned sharply southwards. This instant of abrupt change marks the initial phase of a magnetic storm associated with a sudden decrease in the magnetospheric convective electric field $E_M$ (**Figure 5(b)**) due to the northern rotation of the IMF-$B_z$ [40] [86] [87].

Immediately after ICME_2 at 18:40 UT on June 22 marked by an exceptional SSC with an amplitude of SYM/H = ~2084 nT, while the auroral electrojet continued to progress in a strong increase, a major geomagnetic storm began. During its main phase, storm underwent rapid development in two stages: a first moderate peak was recorded on June 22 at 20:17 UT with an intensity of SYM/H = −138

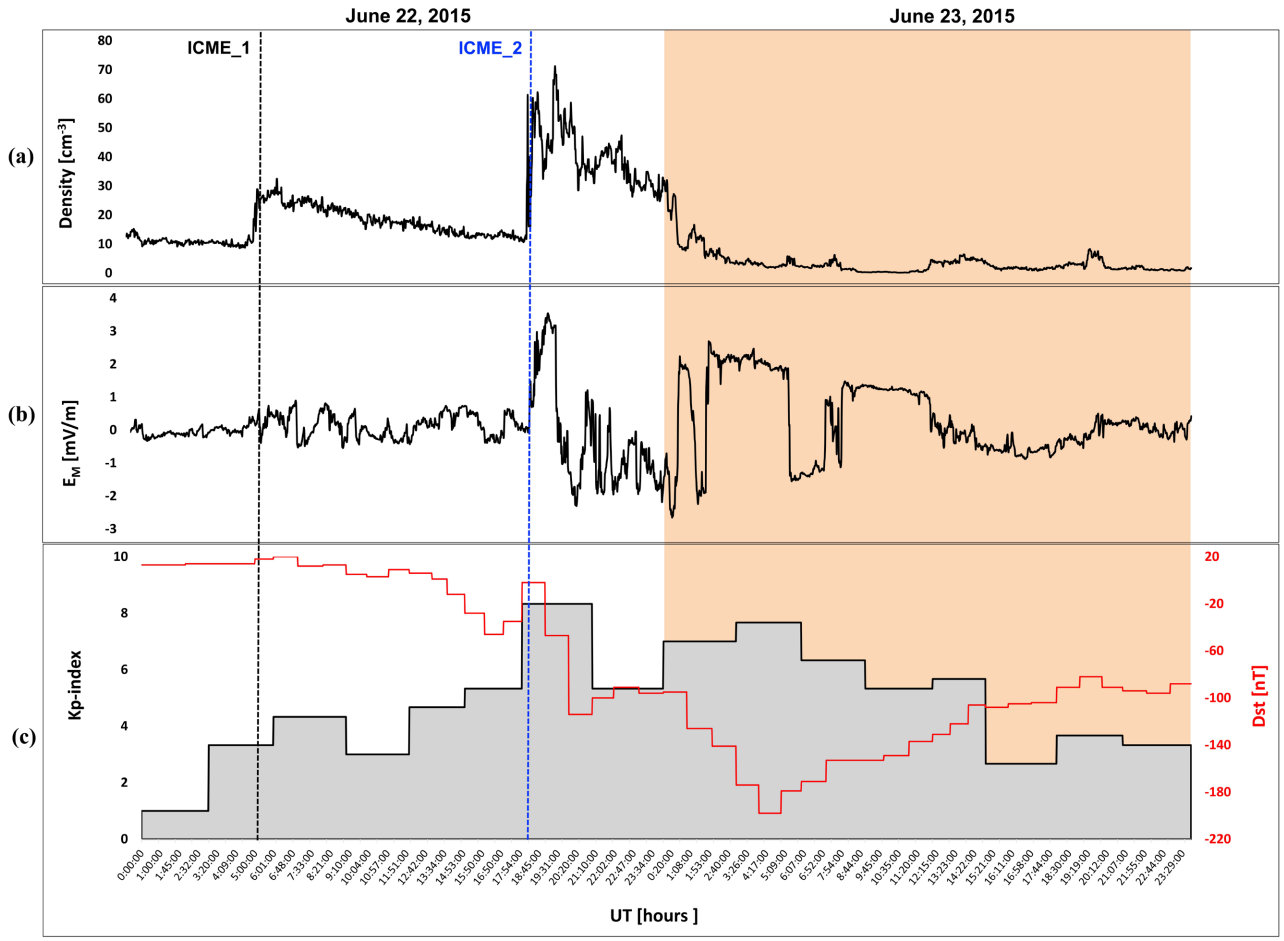


**Figure 5.** Variation of solar and magnetic parameters during the solar events of June 22/23, 2015: (a) Solar flux density; (b) Magnetospheric convection electric field; (c) Magnetic indices Dst and interplanetary Kp.

nT; and a second peak of SYM/H = −208 nT was observed at 04:24 UT the following day (see **Figure 3(d)**, red curve). We believe that two stages in the main phase of the storm are justified by the fact that magnetic fields were oriented towards the south both in the sheath for ICME_1 ($B_z$ very close to 0) and in the solar ejecta for ICME_2. According to several studies [88]-[91], such events are quite common and are caused by two southward-facing field events of roughly equal strength, with the Dst base of the second event (*i.e.*, ICME_2) much lower than that of the first (ICME_1). During this main phase on June 22, a decrease in the horizontal component of the geomagnetic field (SYM/H) was observed. This decrease implies an intensification of the ring current, which controls the electric field inside the magnetosphere at dawn and dusk: magnetospheric convection electric field $E_M$. **Figure 3(c)**, red curve, and **Figure 5(b)**, black curve, show large fluctuations in $E_y$ electric field frozen in solar winds and in $E_M$ field at the beginning of storm's initial phase. These fluctuations become even more pronounced during the storm's main phase. Increasing $E_M$ field fluctuations are clearly associated with negative Dst indices (**Figure 5(c)**, red curve). Indeed, as the Dst index and horizontal component of the Earth's magnetic field SYM/H become more negative during the main phase

of the magnetic storm, the convective electric field $E_M$ becomes more fluctuating. BOX magnetometer (**Figure 3(a)**, red curve) is more sensitive to these fluctuations than DRV (**Figure 3(a)**, black curve). As BOX is at high latitude (close to the Earth's magnetic poles, where the lines are oriented vertically), BOX consequently shows more pronounced effects, indicating greater sensitivity of high-latitude regions to solar wind interactions. We can therefore suggest that during the main phase of geomagnetic storms, the variability $E_M$ field becomes more pronounced and direct in high-latitude regions as solar winds interact with the Earth's magnetic field. [92] reveals that $E_M$ field varies as a function of magnetic latitude, local magnetic time, IMF orientation, and storm season. According to [93], the strongest manifestations of solar wind/magnetosphere system interactions are particularly evident at auroral and polar latitudes. It is important to note that the storm's main phase lasted almost half a day and is characterized by significant electrodynamic effects. The second peak of SYM/H = −208 nT ends the main phase of the storm [18] [61] [80] [94] [95].

Furthermore, the recovery phase (the longest phase of all) of the storm, characterized by an increase in SYM/H due to magnetospheric currents associated with a southerly orientation of IMF-$B_z$, began on June 23 at 04:25 UT and then progressed slowly over the rest of the day. This slowness is due to the fact that all solar wind conditions were constant during June 23, 2015 (see, for example, [19]). Note that IMF-$B_z$ turned north ~01:15 UT after the start of the recovery phase. Earlier estimates by [96] indicated delays of ≈1 - 2 hours. Just before the start of the recovery phase, there is a rapid decrease in $E_M$ field (**Figure 5(b)**) due to the northward orientation or weakening of the southern component of the IMF-$B_z$ (**Figure 3(c)**, black curve). This result is consistent with previous observations [40] [97]. Inversion of IMF-$B_z$ (and therefore of the $E_M$ field since both evolve in phase opposition, [98]) has been identified as an over-shielding electric field [99]-[101]. During the recovery period, over-shielding of the $E_M$ field is driven by the northward orientation of IMF-$B_z$ (e.g., [40] [43]). An important $E_M$ field remark must be made about the dawn-dusk sectors downstream of ICME_2. Indeed, according to **Figure 3(c)** and **Figure 5(b)**, $E_M$ field intensifies in the dawn and dusk sectors in the inner magnetosphere on June 23 for a south-facing IMF-$B_z$. However, for a north-facing IMF-$B_z$, $E_M$ field intensity weakens around 04:20 UT and 04:30 UT, marking a clear difference between the main and recovery phases of the storm. According to [102], when $E_M$ suddenly increases due to a southward rotation of IMF-$B_z$, the result will be a dawn-to-dusk $E_M$ field in the inner magnetosphere. On the other hand, if IMF-$B_z$ rotates northwards, convection diminishes, and there is suddenly a reversed $E_M$ field (from dusk to dawn). [103] and [104] have shown that in the dawn sector, $E_M$ field turns westwards at night, while in the dusk sector, it turns eastwards during the day. While the westward $E_M$ field in the midnight sector was reported by [105], we report here that the eastward and westward $E_M$ field is associated with the orientation of IMF-$B_z$. More clearly, East/West orientations of the dawn-dusk/dusk-dawn electric field during the day/night are associated with a sudden intensification/decrease of the $E_M$ field due to South/North

rotations of the IMF-$B_z$. Note that during the storm's recovery period, several peaks in auroral activity are evident, with its maximum value of around 1795 nT reached around 12:15 UT, as can be seen in **Figure 3(d)**, grey bar. However, after the arrival of ICME_2, there was a notable increase in auroral activity, reaching its highest point of ~2698 nT on June 22 at 20:09 UT. This increase is due to the North/South fluctuations of IMF-$B_z$, indicating sub-storm activity. The presence of two peaks in the AE index indicates that the most intense auroral activity occurred after ICME_2. Intensification of AE suggests a strong, rapid penetration of the auroral electric field towards low latitudes due to substorm activity during the recorded geomagnetic storm. Magnetic substorming occurs when ICME/magnetosphere interaction leads to repeated cycles of magnetic field buildup in magnetotail lobes, cross-current enhancement, and disruption [106] [107].

Moreover, analysis of **Figure 3(b)** shows that ICME_2 caused very large velocity amplitudes in the solar wind on June 23. According to **Figure 5(b)**, these strong amplitudes caused an increase in magnetospheric plasma convection, thus enhancing the SSC signature [108]. Solar wind has an average velocity of 625.80 km/s, and the embedded magnetic field is around 1.57 nT. IMF-$B_z$ intensity of 1.92 nT was predominantly meridional. [19] [109] [110] have proven that the magnetic storm triggered on June 22, 2015 was major. During its main phase, magnetic ($B_z$) and electric ($E_y$) fields exhibited very high amplitudes. [96] describes these high magnetic fields as components of fast ICMEs (speeds > 500 km·s$^{-1}$) originating from the Sun. Strong electric fields within Earth's magnetosphere also provide evidence of strong magnetospheric plasma convection, as can be seen both in **Figure 5(b)** and in [111]. These interplanetary signatures are responsible for sharp decreases in the Dst index (**Figure 5(c)**, red line). As a reminder, the Dst index provides an overview of the effectivity of magnetic storms while excluding auroral phenomena [112]. In this study, Dst recorded observations similar to those of the SYM/H component (**Figure 3(d)** and **Figure 5(c)**, red curves) with a high correlation of 97.79%. Although it seems that Dst and SYM/H are calculated in similar ways, these two indices are totally different in terms of the number of stations used and their temporal resolution. The high correlation found here shows that their meteorological phenomena are not dissociated, as both measure geomagnetic field variations due to ring currents. This storm had a −Dst maximum of 198 nT from 04:00 UT to 04:59 UT, achieved on June 23, 2015. The high intensity (198 nT) of the storm can be explained by the two stages of development during the main phase discussed above. According to **Figure 5(c)**, the magnetic activity index Kp reached a value of 8, *i.e.*, one less than the maximum, which is 9 on the logarithmic scale. Consequently, the June 22-23 storm would be slightly smaller than the St. Patrick's Day storm of March 17, 2015.

## 4. Conclusion

During the filamentary eruptions of June 22 and 23, 2015, one-minute cadence data from ground-based magnetometers and satellite observations were analyzed in this manuscript to further our understanding of the response of Earth's mag-

netosphere to violent geomagnetic storms. Several interesting features were recorded when two interplanetary coronal mass ejections ICMEs (ICME_1 and ICME_2) bombarded the Earth at 05:45 UT and 18:40 UT on June 22. While it appears that the dynamics of the Earth's magnetosphere were significantly affected by the interaction with the selected ICMEs, ICME_2 showed more significant effects on the magnetosphere on both the day and night sides. Analysis of the one-minute cadence data highlighted the important role played by electric field orientations associated with ICME-$B_z$ polarities during the period/phase of extreme storms. Thus, the East/West directions of the dawn-dusk/dusk-dawn electric field during the day/night are associated with a sudden intensification/decrease of the convection electric field due to the South/North rotations of the IMF-$B_z$. While the main phase of the storm is characterized by an electric convection field that becomes strong and positive towards the east during the daytime hours and towards the west during the night hours, the recovery phase is highlighted by a negative component of the electric convection field towards the west during the day and towards the east during the night. The configuration of the magnetospheric convection electric field during the main phase of the storm could be related to the established dawn-dusk convection cycle. Between the two storm phases, our results show a transition characterized by a weakening of the magnetospheric electric field. However, some complex areas remain to be studied, where the same weaknesses in the electric convection field have been observed but do not seem to mark any transition, which could be one of the perspectives of this study. The results obtained in this work are important because, primarily, geomagnetic storms modulate ionospheric electron density and affect the global atmospheric electrical circuit, which has an impact on radio signal propagation. Furthermore, this study could contribute to refining space weather models by improving our understanding of the influence of electric fields on the magnetosphere during geomagnetic storms. However, the main limitation of this work lies in the small sample size considered or the particular structure of this event with two ICMEs. This limitation makes it difficult to generalize our results to other studies. We believe that extending the sampling of severe storms to a larger scale could yield more meaningful results for meteorological decision-making purposes.

## Acknowledgements

The authors would like to thank OMNIWeb "https://omniweb.gsfc.nasa.gov/ow_min.html", ISGI "http://isgi.unistra.fr/", and BCMT "http://www.bcmt.fr/data_download.php" for the data.

## Conflicts of Interest

The authors declare no conflicts of interest regarding the publication of this paper.

## References

[1] Koskinen, H., Tanskanen, E., Pirjola, R., Pulkkinen, A., Dyer, C., Rodgers, D., Can-

non, P., Mandeville, J.-C. and Boscher, D. (2001) Space Weather Effects Catalogue. ESA Space Weather Study (ESWS). http://www.spaceweather.org/ISES/swxeff/1.pdf

[2] Lakhina, G.S. and Tsurutani, B.T. (2016) Geomagnetic Storms: Historical Perspective to Modern View. *Geoscience Letters*, **3**, Article No. 5. https://doi.org/10.1186/s40562-016-0037-4

[3] Schwenn, R. (2006) Space Weather: The Solar Perspective. *Living Reviews in Solar Physics*, **3**, Article No. 2. https://doi.org/10.12942/lrsp-2006-2

[4] Maghrabi, A.H. and Marwa, A.M. (2020) The Effects of Solar Activity and Geomagnetic Disturbance on Human Health. *Open Access Journal of Biomedical Science*, **2**, 506-509. https://doi.org/10.38125/oajbs.000203

[5] Hapgood, M., Angling, M.J., Attrill, G., Bisi, M., Cannon, P.S., Dyer, C., *et al.* (2021) Development of Space Weather Reasonable Worst-Case Scenarios for the UK National Risk Assessment. *Space Weather*, **19**, e2020SW002593. https://doi.org/10.1029/2020sw002593

[6] Srivastava, N. (2006) The Challenge of Predicting the Occurrence of Intense Storms. *Journal of Astrophysics and Astronomy*, **27**, 237-242. https://doi.org/10.1007/bf02702526

[7] Gopalswamy, N., Yashiro, S. and Akiyama, S. (2007) Geoeffectiveness of Halo Coronal Mass Ejections. *Journal of Geophysical Research*: *Space Physics*, **112**, A06112. https://doi.org/10.1029/2006ja012149

[8] Dumbović, M., Devos, A., Vršnak, B., Sudar, D., Rodriguez, L., Ruždjak, D., *et al.* (2014) Geoeffectiveness of Coronal Mass Ejections in the SOHO Era. *Solar Physics*, **290**, 579-612. https://doi.org/10.1007/s11207-014-0613-8

[9] Gosling, J.T., Bame, S.J., McComas, D.J., Phillips, J.L., Pizzo, V.J., Goldstein, B.E., *et al.* (1993) Latitudinal Variation of Solar Wind Corotating Stream Interaction Regions: Ulysses. *Geophysical Research Letters*, **20**, 2789-2792. https://doi.org/10.1029/93gl03116

[10] Harrison, R.A. (1996) Coronal Magnetic Storms: A New Perspective on Flares and the 'Solar Flare Myth'Debate. *Solar Physics*, **166**, 441-444. https://doi.org/10.1007/bf00149411

[11] Cliver, E.W. and Hudson, H.S. (2002) CMEs: How Do the Puzzle Pieces Fit Together? *Journal of Atmospheric and Solar- Terrestrial Physics*, **64**, 231-252. https://doi.org/10.1016/s1364-6826(01)00086-4

[12] Gopalswamy, N. (2006) Coronal Mass Ejections of Solar Cycle 23. *Journal of Astrophysics and Astronomy*, **27**, 243-254. https://doi.org/10.1007/bf02702527

[13] Iyer, K.N., Jadav, R.M., Jadeja, A.K., Manoharan, P.K., Sharma, S. and Vats, H.O. (2006) Space Weather Effects of Coronal Mass Ejection. *Journal of Astrophysics and Astronomy*, **27**, 219-226. https://doi.org/10.1007/bf02702524

[14] Mittal, N. and Narain, U. (2015) On the Arrival Times of Halo Coronal Mass Ejections in the Vicinity of the Earth. *NRIAG Journal of Astronomy and Geophysics*, **4**, 100-105. https://doi.org/10.1016/j.nrjag.2015.05.001

[15] Streltsov, A.V. and Foster, J.C. (2004) Electrodynamics of the Magnetosphere-Ionosphere Coupling in the Nightside Subauroral Zone. *Physics of Plasmas*, **11**, 1260-1267. https://doi.org/10.1063/1.1647139

[16] Saiz, E., Cerrato, Y., Cid, C., Dobrica, V., Hejda, P., Nenovski, P., *et al.* (2013) Geomagnetic Response to Solar and Interplanetary Disturbances. *Journal of Space Weather and Space Climate*, **3**, A26. https://doi.org/10.1051/swsc/2013048

[17] Piersanti, M., Del Moro, D., Parmentier, A., Martucci, M., Palma, F., Sotgiu, A., *et al.*

(2022) On the Magnetosphere-Ionosphere Coupling during the May 2021 Geomagnetic Storm. *Space Weather*, **20**, e2021SW003016. https://doi.org/10.1029/2021sw003016

[18] Astafyeva, E., Zakharenkova, I. and Alken, P. (2016) Prompt Penetration Electric Fields and the Extreme Topside Ionospheric Response to the June 22-23, 2015 Geomagnetic Storm as Seen by the Swarm Constellation. *Earth, Planets and Space*, **68**, Article No. 152. https://doi.org/10.1186/s40623-016-0526-x

[19] Singh, R. and Sripathi, S. (2017) Ionospheric Response to 22-23 June 2015 Storm as Investigated Using Ground-Based Ionosondes and GPS Receivers over India. *Journal of Geophysical Research: Space Physics*, **122**, 645-11, 664. https://doi.org/10.1002/2017ja024460

[20] Şentürk, E. (2020) Investigation of Global Ionospheric Response of the Severe Geomagnetic Storm on June 22-23, 2015 by GNSS-Based TEC Observations. *Astrophysics and Space Science*, **365**, Article No. 110. https://doi.org/10.1007/s10509-020-03828-z

[21] Feng, J., Zhou, Y., Zhou, Y., Gao, S., Zhou, C., Tang, Q., *et al.* (2021) Ionospheric Response to the 17 March and 22 June 2015 Geomagnetic Storms over Wuhan Region Using GNSS-Based Tomographic Technique. *Advances in Space Research*, **67**, 111-121. https://doi.org/10.1016/j.asr.2020.10.008

[22] Tsurutani, B.T., Gonzalez, W.D., Tang, F., Akasofu, S.I. and Smith, E.J. (1988) Origin of Interplanetary Southward Magnetic Fields Responsible for Major Magnetic Storms near Solar Maximum (1978-1979). *Journal of Geophysical Research: Space Physics*, **93**, 8519-8531. https://doi.org/10.1029/ja093ia08p08519

[23] Tsurutani, B.T., Gonzalez, W.D., Tang, F. and Lee, Y.T. (1992) Great Magnetic Storms. *Geophysical Research Letters*, **19**, 73-76. https://doi.org/10.1029/91gl02783

[24] Mcpherron, R.L. (1991) Physical Processes Producing Magnetospheric Substorms and Magnetic Storms. *Geomagnetism*, **4**, 593-739. https://doi.org/10.1016/b978-0-12-378674-6.50013-3

[25] Tsurutani, B.T., Gonzalez, W.D., Guarnieri, F., Kamide, Y., Zhou, X. and Arballo, J.K. (2004) Are High-Intensity Long-Duration Continuous AE Activity (HILDCAA) Events Substorm Expansion Events? *Journal of Atmospheric and Solar-Terrestrial Physics*, **66**, 167-176. https://doi.org/10.1016/j.jastp.2003.08.015

[26] Lakhina, G.S., Alex, S., Mukherjee, S. and Vichare, G. (2006) On Magnetic Storms and Substorms. I*LWS WORKSHOP* 2006, Goa, 19-24 February 2006, 1-8.

[27] Gonzalez, W.D., Joselyn, J.A., Kamide, Y., Kroehl, H.W., Rostoker, G., Tsurutani, B.T., *et al.* (1994) What Is a Geomagnetic Storm? *Journal of Geophysical Research: Space Physics*, **99**, 5771-5792. https://doi.org/10.1029/93ja02867

[28] Tsurutani, B.T., Gonzalez, W.D., Gonzalez, A.L.C., Tang, F., Arballo, J.K. and Okada, M. (1995) Interplanetary Origin of Geomagnetic Activity in the Declining Phase of the Solar Cycle. *Journal of Geophysical Research: Space Physics*, **100**, 21717-21733. https://doi.org/10.1029/95ja01476

[29] Nishimura, Y., Shinbori, A., Ono, T., Iizima, M. and Kumamoto, A. (2006) Storm-time Electric Field Distribution in the Inner Magnetosphere. *Geophysical Research Letters*, **33**, L22102. https://doi.org/10.1029/2006gl027510

[30] Bhaskar, A. and Vichare, G. (2019) Forecasting of SYMH and ASYH Indices for Geomagnetic Storms of Solar Cycle 24 Including St. Patrick's Day, 2015 Storm Using NARX Neural Network. *Journal of Space Weather and Space Climate*, **9**, A12. https://doi.org/10.1051/swsc/2019007

[31] Imtiaz, N., Younas, W. and Khan, M. (2020) Response of the Low- to Mid-Latitude

Ionosphere to the Geomagnetic Storm of September 2017. *Annales Geophysicae*, **38**, 359-372. https://doi.org/10.5194/angeo-38-359-2020

[32] Silwal, A., Gautam, S.P., Poudel, P., Karki, M., Chapagain, N.P. and Adhikari, B. (2023) Variation of Total Electron Content over Nepal during Geomagnetic Storms: GPS Observations. *Russian Journal of Earth Sciences*, **23**, ES3012. https://doi.org/10.2205/2023es000833

[33] Armando C-V., Pablo M. and Cid C. (2024) Operational SYM-H Forecasting with Confidence Intervals Using Deep Neural Networks. *Space Weather*, **22**, e2024SW004039. https://doi.org/10.1029/2024sw004039

[34] Amin, E.A., Shaltout, A.M.K., Abdelkawy, A.G.A., Beheary, M.M., Abdelhamid, R. and Shimeis, A. (2025) The Influence of Solar Activity on Geomagnetic Disturbances over Cycles 23 and 24. *Advances in Space Research*, **75**, 6553-6570. https://doi.org/10.1016/j.asr.2025.02.030

[35] Spiro, R.W., Wolf, R.A. and Fejer, B.G. (1988) Penetration of High-Latitude-Electric-Field Effects to Low Latitudes during Sundial 1984. *Annals of Geophysics*, **6**, 39-50.

[36] (2007) Solar Atmosphere. In: Kamide, Y., Chian, A., Eds., *Handbook of the Solar-Terrestrial Environment*, Springer, 55-93.

[37] Araki, T., Allen, J.H. and Araki, Y. (1985) Extension of a Polar Ionospheric Current to the Nightside Equator. *Planetary and Space Science*, **33**, 11-16. https://doi.org/10.1016/0032-0633(85)90137-0

[38] Sastri, J.H. (1988) Equatorial Electric Fields of Ionospheric Disturbance Dynamo Origin. *Annals of Geophysics*, **6**, 635-642.

[39] Kikuchi, T., Lühr, H., Kitamura, T., Saka, O. and Schlegel, K. (1996) Direct Penetration of the Polar Electric Field to the Equator during a DP 2 Event as Detected by the Auroral and Equatorial Magnetometer Chains and the EISCAT Radar. *Journal of Geophysical Research*: *Space Physics*, **101**, 17161-17173. https://doi.org/10.1029/96ja01299

[40] Kikuchi, T., Hashimoto, K.K. and Nozaki, K. (2008) Penetration of Magnetospheric Electric Fields to the Equator during a Geomagnetic Storm. *Journal of Geophysical Research*: *Space Physics*, **113**, A06214. https://doi.org/10.1029/2007ja012628

[41] Abdu, M.A., Nogueira, P.A.B., Santos, A.M., de Souza, J.R., Batista, I.S. and Sobral, J.H.A. (2018) Impact of Disturbance Electric Fields in the Evening on Prereversal Vertical Drift and Spread F Developments in the Equatorial Ionosphere. *Annales Geophysicae*, **36**, 609-620. https://doi.org/10.5194/angeo-36-609-2018

[42] Singh, R., Lee, Y.S., Song, S.M., Kim, Y.H., Yun, J.Y., Sripathi, S., *et al.* (2022) Ionospheric Density Oscillations Associated with Recurrent Prompt Penetration Electric Fields during the Space Weather Event of 4 November 2021 over the East-Asian Sector. *Journal of Geophysical Research*: *Space Physics*, **127**, e2022JA030456. https://doi.org/10.1029/2022ja030456

[43] Huang, C., Foster, J.C. and Kelley, M.C. (2005) Long-Duration Penetration of the Interplanetary Electric Field to the Low-latitude Ionosphere during the Main Phase of Magnetic Storms. *Journal of Geophysical Research*: *Space Physics*, **110**, A11309. https://doi.org/10.1029/2005ja011202

[44] Mannucci, A.J., Tsurutani, B.T., Iijima, B.A., Komjathy, A., Saito, A., Gonzalez, W.D., *et al.* (2005) Dayside Global Ionospheric Response to the Major Interplanetary Events of October 29-30, 2003 "Halloween Storms". *Geophysical Research Letters*, **32**, L12S02-L12. https://doi.org/10.1029/2004gl021467

[45] Tsurutani, B.T., Verkhoglyadova, O.P., Mannucci, A.J., Saito, A., Araki, T., Yumoto,

K., *et al.* (2008) Prompt Penetration Electric Fields (PPEFs) and Their Ionospheric Effects during the Great Magnetic Storm of 30-31 October 2003. *Journal of Geophysical Research*: *Space Physics*, **113**, A05311. https://doi.org/10.1029/2007ja012879

[46] Wei, Y., Zhao, B., Li, G. and Wan, W. (2015) Electric Field Penetration into Earth's Ionosphere: A Brief Review for 2000-2013. *Science Bulletin*, **60**, 748-761. https://doi.org/10.1007/s11434-015-0749-4

[47] Nilam, B., Ram, S.T., Shiokawa, K., Balan, N. and Zhang, Q. (2020) The Solar Wind Density Control on the Prompt Penetration Electric Field and Equatorial Electrojet. *Journal of Geophysical Research*: *Space Physics*, **125**, e2020JA027869. https://doi.org/10.1029/2020ja027869

[48] Astafyeva, E., Zakharenkova, I., Huba, J.D., Doornbos, E. and van den IJssel, J. (2017) Global Ionospheric and Thermospheric Effects of the June 2015 Geomagnetic Disturbances: Multi-Instrumental Observations and Modeling. *Journal of Geophysical Research*: *Space Physics*, **122**, 11716-11742. https://doi.org/10.1002/2017ja024174

[49] Tsugawa, T., Saito, A., Otsuka, Y. and Yamamoto, M. (2003) Damping of Large-Scale Traveling Ionospheric Disturbances Detected with GPS Networks during the Geomagnetic Storm. *Journal of Geophysical Research*: *Space Physics*, **108**, Article No. 1127. https://doi.org/10.1029/2002ja009433

[50] Liu, H. and Lühr, H. (2005) Strong Disturbance of the Upper Thermospheric Density Due to Magnetic Storms: CHAMP Observations. *Journal of Geophysical Research*: *Space Physics*, **110**, A09S29. https://doi.org/10.1029/2004ja010908

[51] Foster, J.C. and Coster, A.J. (2007) Conjugate Localized Enhancement of Total Electron Content at Low Latitudes in the American Sector. *Journal of Atmospheric and Solar-Terrestrial Physics*, **69**, 1241-1252. https://doi.org/10.1016/j.jastp.2006.09.012

[52] Balan, N., Yamamoto, M., Liu, J.Y., Otsuka, Y., Liu, H. and Lühr, H. (2011) New Aspects of Thermospheric and Ionospheric Storms Revealed by Champ. *Journal of Geophysical Research*: *Space Physics*, **116**, A07305. https://doi.org/10.1029/2010ja016399

[53] Afraimovich, E.L., Astafyeva, E.I., Demyanov, V.V., Edemskiy, I.K., Gavrilyuk, N.S., Ishin, A.B., *et al.* (2013) A Review of GPS/GLONASS Studies of the Ionospheric Response to Natural and Anthropogenic Processes and Phenomena. *Journal of Space Weather and Space Climate*, **3**, A27. https://doi.org/10.1051/swsc/2013049

[54] Lei, J., Wang, W., Burns, A.G., Yue, X., Dou, X., Luan, X., *et al.* (2014) New Aspects of the Ionospheric Response to the October 2003 Superstorms from Multiple-Satellite Observations. *Journal of Geophysical Research*: *Space Physics*, **119**, 2298-2317. https://doi.org/10.1002/2013ja019575

[55] Nayak, C., Tsai, L.-C., Su, S.-Y., Galkin, I.A., Tan, A.T.K., Nofri, E., *et al.* (2016) Peculiar Features of the Low-Latitude and Midlatitude Ionospheric Response to the St. Patrick's Day Geomagnetic Storm of 17 March 2015. *Journal of Geophysical Research*: *Space Physics*, **121**, 7941-7960. https://doi.org/10.1002/2016ja022489

[56] Zhong, J., Wang, W., Yue, X., Burns, A.G., Dou, X. and Lei, J. (2016) Long-Duration Depletion in the Topside Ionospheric Total Electron Content during the Recovery Phase of the March 2015 Strong Storm. *Journal of Geophysical Research*: *Space Physics*, **121**, 4733-4747. https://doi.org/10.1002/2016ja022469

[57] Lei, W., Gendrin, R., Higel, B. and Berchem, J. (1981) Relationships between the Solar Wind Electric Field and the Magnetospheric Convection Electric Field. *Geophysical Research Letters*, **8**, 1099-1102. https://doi.org/10.1029/gl008i010p01099

[58] Bouvet, J. and Lafeuille, M. (1982) Bibliographie du sondeur français à diffusio nincohérente (1962-1982). Centre de recherches en physique de l'environnement terrestre et

planétaire (CRPE), 220. https://hal-lara.archives-ouvertes.fr/hal-02191788v1

[59] Dayeh, M.A. (2015) Coronal Mass Ejections. In: Pelton, J. and Allahdadi, F., Eds., *Handbook of Cosmic Hazards and Planetary Defense*, Springer International Publishing, 81-98. https://doi.org/10.1007/978-3-319-03952-7_9

[60] Gnanou, I., Kabore, S., Gyebre, A.M.F., Zoundi, C., Zerbo, J. and Ouattara, F. (2023) Effect of High-Speed Solar Winds Turbulence Upstream of the Earth's Magnetosphere: Case of the Outer Minima of Solar Cycles 20, 21, 22, 23 and 24. *Open Journal of Applied Sciences*, **13**, 1145-1162. https://doi.org/10.4236/ojapps.2023.137091

[61] Liu, Y.D., Hu, H., Wang, R., Yang, Z., Zhu, B., Liu, Y.A., *et al.* (2015) Plasma and Magnetic Field Characteristics of Solar Coronal Mass Ejections in Relation to Geomagnetic Storm Intensity and Variability. *The Astrophysical Journal*, **809**, L34. https://doi.org/10.1088/2041-8205/809/2/l34

[62] Huba, J.D. and Sazykin, S. (2014) Storm Time Ionosphere and Plasmasphere Structuring: SAMI3-RCM Simulation of the 31 March 2001 Geomagnetic Storm. *Geophysical Research Letters*, **41**, 8208-8214. https://doi.org/10.1002/2014gl062110

[63] Huba, J.D., Sazykin, S. and Coster, A. (2017) SAMI3-RCM Simulation of the 17 March 2015 Geomagnetic Storm. *Journal of Geophysical Research*: *Space Physics*, **122**, 1246-1257. https://doi.org/10.1002/2016ja023341

[64] Kikuchi, T. and Hashimoto, K.K. (2016) Transmission of the Electric Fields to the Low Latitude Ionosphere in the Magnetosphere-Ionosphere Current Circuit. *Geoscience Letters*, **3**, 1-11. https://doi.org/10.1186/s40562-016-0035-6

[65] Kappenman, J.G. (2001) An Introduction to Power Grid Impacts and Vulnerabilities from Space Weather. In: Daglis, I.A., Ed., *Space Storms and Space Weather Hazards*, Springer, 335-361. https://doi.org/10.1007/978-94-010-0983-6_13

[66] Astafyeva, E., Yasyukevich, Y., Maksikov, A. and Zhivetiev, I. (2014) Geomagnetic Storms, Super-Storms, and Their Impacts on GPS-Based Navigation Systems. *Space Weather*, **12**, 508-525. https://doi.org/10.1002/2014sw001072

[67] Cherniak, I. and Zakharenkova, I. (2016) First Observations of Super Plasma Bubbles in Europe. *Geophysical Research Letters*, **43**, 137-11, 145. https://doi.org/10.1002/2016gl071421

[68] Astafyeva, E., Zakharenkova, I., Hozumi, K., Alken, P., Coïsson, P., Hairston, M.R., *et al.* (2018) Study of the Equatorial and Low-Latitude Electrodynamic and Ionospheric Disturbances during the 22-23 June 2015 Geomagnetic Storm Using Ground-based and Spaceborne Techniques. *Journal of Geophysical Research*: *Space Physics*, **123**, 2424-2440. https://doi.org/10.1002/2017ja024981

[69] Uga, C.I., Gautam, S.P. and Seba, E.B. (2024) TEC Disturbances Caused by CME-Triggered Geomagnetic Storm of September 6-9, 2017. *Heliyon*, **10**, e30725. https://doi.org/10.1016/j.heliyon.2024.e30725

[70] Morton, Y.J., Yang, Z., Breitsch, B., Bourne, H. and Rino, C. (2020) Ionospheric Effects, Monitoring, and Mitigation Techniques. In: Jade Morton, Y.T., van Diggelen, F., Spilker Jr., J.J., Parkinson, B.W., Lo, S. and Gao G., Eds., *Position*, *Navigation*, *and Timing Technologies in the 21st Century*, John Wiley Sons, Ltd., 879-937.

[71] Luo, X., Du, J., Lou, Y., Gu, S., Yue, X., Liu, J., *et al.* (2022) A Method to Mitigate the Effects of Strong Geomagnetic Storm on GNSS Precise Point Positioning. *Space Weather*, **20**, e2021SW002908. https://doi.org/10.1029/2021sw002908

[72] Shen, Y., Verkhoglyadova, O.P., Artemyev, A., Hartinger, M.D., Angelopoulos, V., Shi, X., *et al.* (2024) Magnetospheric Control of Ionospheric TEC Perturbations via Whistler-Mode and ULF Waves. *AGU Advances*, **5**, e2024AV001302.

https://doi.org/10.1029/2024av001302

[73] Shugay, Y., Slemzin, V. and Veselovsky, I. (2014) Magnetic Field Sector Structure and Origins of Solar Wind Streams in 2012. *Journal of Space Weather and Space Climate*, **4**, A24. https://doi.org/10.1051/swsc/2014021

[74] Berezin, I. and Tlatov, A. (2022) Coronal Field Geometry and Solar Wind Speed. *Universe*, **8**, Article 646. https://doi.org/10.3390/universe8120646

[75] Birch, M.J. (2025) On the Determination of the Speed of a Fast Solar Wind Stream Using Two Independent Measurements of the Interplanetary Magnetic Field. *Annals of Mathematics and Physics*, **8**, 35-44. https://doi.org/10.17352/amp.000144

[76] Fejer, B.G., Jensen, J.W., Kikuchi, T., Abdu, M.A. and Chau, J.L. (2007) Equatorial Ionospheric Electric Fields during the November 2004 Magnetic Storm. *Journal of Geophysical Research*: *Space Physics*, **112**, A10304. https://doi.org/10.1029/2007ja012376

[77] Verkhoglyadova, O.P., Tsurutani, B.T., Mannucci, A.J., Saito, A., Araki, T., Anderson, D., *et al.* (2013) Simulation of PPEF Effects in Dayside Low-Latitude Ionosphere for the October 30, 2003, Superstorm. In: Kintner, P., *et al.*, Eds., *Geophysical Monograph Series*, American Geophysical Union, 169-177. https://doi.org/10.1029/181gm16

[78] Biktash, L.S. (2008) The Solar Wind Energy Input Rate and Recovery of the Magnetospheric Ring Current during the Last Two Solar Cycles. *Sun and Geosphere*, **3**, 46-51.

[79] Piersanti, M., Alberti, T., Bemporad, A., Berrilli, F., Bruno, R., Capparelli, V., *et al.* (2017) Comprehensive Analysis of the Geoeffective Solar Event of 21 June 2015: Effects on the Magnetosphere, Plasmasphere, and Ionosphere Systems. *Solar Physics*, **292**, Article No. 169. https://doi.org/10.1007/s11207-017-1186-0

[80] Le, G., Chi, P.J., Strangeway, R.J., Russell, C.T., Slavin, J.A., Takahashi, K., *et al.* (2017) Global Observations of Magnetospheric High-*m* Poloidal Waves during the 22 June 2015 Magnetic Storm. *Geophysical Research Letters*, **44**, 3456-3464. https://doi.org/10.1002/2017gl073048

[81] Watari, S. (2017) Geomagnetic Storms of Cycle 24 and Their Solar Sources. *Earth, Planets and Space*, **69**, Article No. 10. https://doi.org/10.1186/s40623-017-0653-z

[82] Maurya, A.K., Venkatesham, K., Kumar, S., Singh, R., Tiwari, P. and Singh, A.K. (2018) Effects of St. Patrick's Day Geomagnetic Storm of March 2015 and of June 2015 on Low-Equatorial *d* Region Ionosphere. *Journal of Geophysical Research*: *Space Physics*, **123**, 6836-6850. https://doi.org/10.1029/2018ja025536

[83] Habyarimana, V., Habarulema, J.B. and Dugassa, T. (2023) Analysis of Ionospheric Storm-Time Effects over the East African Sector during the 17 March 2013 and 2015 Geomagnetic Storms. *Earth, Planets and Space*, **75**, Article No. 58. https://doi.org/10.1186/s40623-023-01812-9

[84] Hashimoto, K.K., Kikuchi, T., Tomizawa, I., Hosokawa, K., Chum, J., Buresova, D., *et al.* (2020) Penetration Electric Fields Observed at Middle and Low Latitudes during the 22 June 2015 Geomagnetic Storm. *Earth, Planets and Space*, **72**, 1-15. https://doi.org/10.1186/s40623-020-01196-0

[85] Ambili, K.M. and Choudhary, R.K. (2023) The Role of the Storm-Time Prompt Penetrating Electric Field on the Net Distribution of Plasma Density over the Low Latitude Ionospheric Regions. *Advances in Space Research*, **72**, 1644-1655. https://doi.org/10.1016/j.asr.2023.04.046

[86] Kobea, A.T., Richmond, A.D., Emery, B.A., Peymirat, C., Lühr, H., Moretto, T., *et al.* (2000) Electrodynamic Coupling of High and Low Latitudes: Observations on May

27, 1993. *Journal of Geophysical Research*: *Space Physics*, **105**, 22979-22989. https://doi.org/10.1029/2000ja000058

[87] Kikuchi, T. (2013) Transmission Line Model for Driving Plasma Convection in the Inner Magnetosphere. In: Pulkkinen, T.I., Tsyganenko, N.A. and Friedel, R.H.W., Eds., *The Inner Magnetosphere*: *Physics and Modeling*, American Geophysical Union, 173-179. https://doi.org/10.1029/155gm20

[88] Grande, M., Perry, C.H., Blake, J.B., Chen, M.W., Fennell, J.F. and Wilken, B. (1996) Observations of Iron, Silicon, and Other Heavy Ions in the Geostationary Altitude Region during Late March 1991. *Journal of Geophysical Research*: *Space Physics*, **101**, 24707-24718. https://doi.org/10.1029/96ja00044

[89] Daglis, I.A. (1997) The Role of Magnetosphere-Ionosphere Coupling in Magnetic Storm Dynamics. In: Tsurutani, B.T., Gonzalez, W.D., Kamide, Y. and Arballo, J.K., Eds, *Magnetic Storms*, American Geophysical Union, 107-116. https://doi.org/10.1029/gm098p0107

[90] Tsurutani, B.T. and Gonzalez, W.D. (1997) The Interplanetary Causes of Magnetic Storms: A Review. In: Tsurutani, B.T., Gonzalez, W.D., Kamide, Y. and Arballo, J.K., Eds, *Magnetic Storms*, American Geophysical Union, 77-89. https://doi.org/10.1029/gm098p0077

[91] Kamide, Y., Yokoyama, N., Gonzalez, W., Tsurutani, B.T., Daglis, I.A., Brekke, A., *et al.* (1998) Two-Step Development of Geomagnetic Storms. *Journal of Geophysical Research*: *Space Physics*, **103**, 6917-6921. https://doi.org/10.1029/97ja03337

[92] Matsuo, T., Richmond, A.D. and Hensel, K. (2003) High-Latitude Ionospheric Electric Field Variability and Electric Potential Derived from DE-2 Plasma Drift Measurements: Dependence on IMF and Dipole Tilt. *Journal of Geophysical Research*: *Space Physics*, **108**, Article 1005. https://doi.org/10.1029/2002ja009429

[93] Victor, N.J., Panneerselvam, C. and Anil Kumar, C.P. (2015) Variation of Surface Electric Field during Geomagnetic Disturbed Period at Maitri, Antarctica. *Journal of Earth System Science*, **124**, 1721-1733. https://doi.org/10.1007/s12040-015-0638-x

[94] Reiff, P.H., Daou, A.G., Sazykin, S.Y., Nakamura, R., Hairston, M.R., Coffey, V., *et al.* (2016) Multispacecraft Observations and Modeling of the 22/23 June 2015 Geomagnetic Storm. *Geophysical Research Letters*, **43**, 7311-7318. https://doi.org/10.1002/2016gl069154

[95] Choraghe, K., Raghav, A., Chakrabarty, D., Kasthurirangan, S. and Bijewar, N. (2021) Properties of the Recovery Phase of Extreme Storms. *Journal of Geophysical Research*: *Space Physics*, **126**, e2020JA028685. https://doi.org/10.1029/2020ja028685

[96] Gonzalez, W.D., Tsurutani, B.T. and Clúa de Gonzalez, A.L. (1999) Interplanetary Origin of Geomagnetic Storms. *Space Science Reviews*, **88**, 529-562. https://doi.org/10.1023/a:1005160129098

[97] Tsuji, Y., Shinbori, A., Kikuchi, T. and Nagatsuma, T. (2012) Magnetic Latitude and Local Time Distributions of Ionospheric Currents during a Geomagnetic Storm. *Journal of Geophysical Research*: *Space Physics*, **117**, A07318. https://doi.org/10.1029/2012ja017566

[98] Gnanou, I., Gyébré, A.M.F., Guibula, K., Zoundi, C. and Ouattara, F. (2022) Energetic Dynamics of the Inner Magnetosphere in Contact with Fast Solar Wind Currents: Case of the Period 1964-2009. *International Journal of Geosciences*, **13**, 329-348. https://doi.org/10.4236/ijg.2022.135018

[99] Fejer, B.G., Gonzales, C.A., Farley, D.T., Kelley, M.C. and Woodman, R.F. (1979) Equatorial Electric Fields during Magnetically Disturbed Conditions 1. The Effect of the Interplanetary Magnetic Field. *Journal of Geophysical Research*: *Space Physics*,

**84**, 5797-5802. https://doi.org/10.1029/ja084ia10p05797

[100] Veenadhari, B., Kikuchi, T., Kumar, S., Tulasiram, S., Chakrabarty, D., Ebihara, Y., *et al.* (2019) Signatures of Substorm Related Overshielding Electric Field at Equatorial Latitudes under Steady Southward IMF BZ during Main Phase of Magnetic Storm. *Advances in Space Research*, **64**, 1975-1988. https://doi.org/10.1016/j.asr.2019.04.001

[101] Vichare, G. and Bagiya, M.S. (2024) Manifestations of Strong IMF-by on the Equatorial Ionospheric Electrodynamics during 10 May 2024 Geomagnetic Storm. *Geophysical Research Letters*, **51**, e2024GL112569. https://doi.org/10.1029/2024gl112569

[102] Goldstein, J., Spiro, R.W., Sandel, B.R., Wolf, R.A., Su, S.-Y. and Reiff, P.H. (2003) Overshielding Event of 28-29 July 2000. *Geophysical Research Letters*, **30**, 1-4. https://doi.org/10.1029/2002gl016644

[103] Jaggi, R.K. and Wolf, R.A. (1973) Self-Consistent Calculation of the Motion of a Sheet of Ions in the Magnetosphere. *Journal of Geophysical Research*, **78**, 2852-2866. https://doi.org/10.1029/ja078i016p02852

[104] Fejer, B.G., Spiro, R.W., Wolf, R.A. and Foster, J.C. (1990) Latitudinal Variation of Perturbation Electric Fields during Magnetically Disturbed Periods: 1986 SUNDI-AL Observations and Model Results. *Annals of Geophysics*, **8**, 441-454.

[105] Sastri, J.H., Niranjan, K. and Subbarao, K.S.V. (2002) Response of the Equatorial Ionosphere in the Indian (Midnight) Sector to the Severe Magnetic Storm of July 15, 2000. *Geophysical Research Letters*, **29**, Article No. 1651. https://doi.org/10.1029/2002gl015133

[106] Birn, J. and Priest, E. (2007) Reconnection of Magnetic Field: Magnetohydrodynamic and Collision Less Theory and Observation. Los Alamos National Laboratory.

[107] Petrukovich, A., Artemyev, A. and Nakamura, R. (2016) Magnetotail Reconnection. In: Gonzalez, W. and Parker, E., Eds., *Astrophysics and Space Science Library*, Springer International Publishing, 277-313. https://doi.org/10.1007/978-3-319-26432-5_7

[108] Fiori, R.A.D., Boteler, D.H. and Gillies, D.M. (2014) Assessment of GIC Risk Due to Geomagnetic Sudden Commencements and Identification of the Current Systems Responsible. *Space Weather*, **12**, 76-91. https://doi.org/10.1002/2013sw000967

[109] Macho, E.P., Correia, E., Paulo, C.M., Angulo, L. and Vieira, J.A.G. (2020) Ionospheric Response to the June 2015 Geomagnetic Storm in the South American Region. *Advances in Space Research*, **65**, 2172-2183. https://doi.org/10.1016/j.asr.2020.02.025

[110] Afolabi, O.O., Candido, C.M.N., Becker-Guedes, F. and Amory-Mazaudier, C. (2024) Study and Modelling of the Impact of June 2015 Geomagnetic Storms on the Brazilian Ionosphere. *Atmosphere*, **15**, Article 597. https://doi.org/10.3390/atmos15050597

[111] Okada, T., Hayakawa, H., Tsuruda, K., Nishida, A. and Matsuoka, A. (1993) EXOS D Observations of Enhanced Electric Fields during the Giant Magnetic Storm in March 1989. *Journal of Geophysical Research*: *Space Physics*, **98**, 15417-15424. https://doi.org/10.1029/93ja01128

[112] Yermolaev, Y.I. and Yermolaev, M.Y. (2006) Statistic Study on the Geomagnetic Storm Effectiveness of Solar and Interplanetary Events. *Advances in Space Research*, **37**, 1175-1181. https://doi.org/10.1016/j.asr.2005.03.130